

Quantitative analysis of a $\text{Fe}_3\text{O}_4 + \text{Li}_x\text{Fe}_3\text{O}_4$ sample by the X-ray Rietveld method

J. RODRÍGUEZ

Instituto de Ciencia de Materiales, CSIC, Martí i Franqués s/n, Barcelona 08028, Spain

J. FONTCUBERTA

Facultat de Física, Universitat de Barcelona, Diagonal 645, Barcelona 08028, Spain

The $\text{Li}_x\text{Fe}_3\text{O}_4$ phase shows a strong peak-overlapping with those of pure magnetite, and a routine X-ray analysis does not allow the detection of the presence of any Fe_3O_4 . However, a careful inspection of the observed calculated difference pattern has led to the deduction of the presence of Fe_3O_4 . This paper shows that the Rietveld method can be used to obtain significant information about the relative concentration of the components of a two-phase sample, even in the case of poor crystallinity, strong overlapping between the diffraction peaks, and only a partially known structure.

1. Introduction

The Rietveld method is largely used for the analysis of neutron diffraction data of polycrystalline materials [1]. In the X-ray case it has not been possible to find an easily-handled analytical expression for the line shape, with some adjustable parameters having physical meaning [2-4]. However, Pearson VII or Pseudo-Voigt functions [3] can be used with satisfactory results in most cases.

In addition to the peak-shape problem, the main disadvantage of X-ray diffraction (XRD) with respect to the neutron case is the lower sensitivity to discriminate elements of close atomic number and the strong preferential orientation of the particles that for most materials, appears when the conventional diffractometers are used in the reflection mode. This last point needs deeper research in order to find useful correction functions and to improve the sample preparation. Despite these difficulties, when one is dealing with complex structures, constraints between parameters or generalized coordinates can be used successfully in both cases [5, 6].

X-ray diffractometers are used much more than neutron reactors and consequently the X-ray case is being extensively investigated in order to extract the maximum information contained in diffraction patterns. In particular, the analysis of patterns containing more than one single phase has not been studied enough, in spite of this some currently available programs include the possibility to perform this kind of refinement in a very straightforward manner [7, 8]. The paper of Bendall and Thomas [8] presents a serious discussion concerning the possibility of a quantitative analysis of mixtures. In summary, it is argued that the strong correlation between the scale factors (or occupation factors) and temperature parameters within and/or between the patterns of each phase, leads to a very high inaccuracy of the relative fraction of each phase. These authors conclude that

the errors in the composition obtained by Werner *et al.* [9] must be multiplied by a factor of two.

In this paper we present a description of the refinements carried out on $\text{Li}_x\text{Fe}_3\text{O}_4$, a material of particular interest for its potential application as a solid-state battery electrode. This compound is specially convenient for performing a test of the multicomponent Rietveld method because its simple structure (spinel-like cubic structure) leads to an important overlapping with the Fe_3O_4 pattern and the unknown parameters to be refined are mainly profile parameters. It should be emphasized that the purpose of this paper is not to solve the structure of $\text{Li}_x\text{Fe}_3\text{O}_4$, which cannot be completely described as a simple cubic spinel structure (see below).

The paper is organized as follows. In Section 2 the experimental details, including synthesis, Mössbauer Spectroscopy and X-ray diffraction are presented. The factors contributing to the scale factors and its use in determining the relative concentration of each phase in a multiphase pattern are also discussed.

In Section 3 a review of the proposed mechanism of lithium incorporation in Fe_3O_4 is given. We present the Rietveld results of the different single-phase models used to illustrate how we have been forced to assume the existence of two phases, which was later confirmed by Mössbauer Spectroscopy. In Section 4, we show the refinements performed with a two-phases model. In Section 5 we summarize the most important conclusions of this study.

2. Experimental and analysis methods

The lithium insertion process has been carried out at room temperature by using *n*-butyl lithium and high-purity Fe_3O_4 . The lithium content of the sample has been determined by atomic absorption, leading to the chemical formula $\text{Li}_{1.7}\text{Fe}_3\text{O}_4$. Further synthesis details can be found elsewhere [10].

The Mössbauer spectrum has been recorded at

room temperature by using a ^{57}Co :Rh source and a 512-channels analyser.

The X-ray diffraction pattern has been recorded between 14° and 100° two-theta values, in a step-scanning mode ($\Delta 2\theta = 0.04^\circ$, $t = 10 \text{ sec step}^{-1}$) with a Siemens D-500 diffractometer, using $\text{CuK}\alpha$ radiation and a pyrolytic graphite diffracted-beam monochromator. A 0.05° slit detector was used leading to the number of counts per step between 30 (background) and 2700 (maximum). The complete pattern profile has been refined by using the DBW3.9 version of the Wiles and Young program [7]. The pseudo-Voigt (p-V) line-shape function was used. However, in all cases the refined η parameter [7] and its standard deviation always included the value corresponding to a simple lorentzian profile. In fact, the lorentzian component of the p-V function should be expected to be dominant if the peak broadening is caused by crystallite-size effects [11].

The determination of the relative concentration of each phase present in the sample has been evaluated from the refined scale factors K_i . It includes the contributions given by the expression:

$$K_i = aV_i/V_{ci}^2\bar{\mu} \quad (1)$$

where a is a constant, common for all of the phases. It contains universal constants and the factors necessary to obtain intensities in an absolute scale. V_i is the irradiated volume of phase i and V_{ci} is the volume of the corresponding unit cell. The linear absorption coefficient $\bar{\mu}$ holds for all the sample. This expression is correct in the approximation of infinite sample thickness, when the absorption factor entering in the diffracted intensity expression is independent of the scattering angle, and when the occupation numbers in the structure-factor calculations are introduced in such a form that $F_i(000)$ gives the correct number of electrons per unit cell for each phase [12].

When two phases are present in the sample, the relative fraction of one of them can be obtained from Equation 1 as:

$$r_{12} = K_1 V_{c1} Z_1 M_1 / K_2 V_{c2} Z_2 M_2 \quad (2)$$

$$x_2 = 100/(1 + r_{12}) \quad (3)$$

where Z_i and M_i are the number of formula units per unit cell and the molecular weight, respectively. In our case, when a secondary phase (magnetite) is included in the refinement, we will assume its cell and all structural parameters except the temperature factor to be known (and fixed). Therefore, the scale factor is the unique fitting-parameter of the secondary phase necessary in order to get its concentration.

The fitting parameters are the usual in the Rietveld method (see [7] for details). We have employed a six-parameter polynomial function to fit the background. The asymmetry correction was included for angles lower than $2\theta = 50^\circ$.

The cycles of refinement were continued until the variation of all the parameters were lower than 0.3 standard deviations.

As mentioned above, in all refinements we have used the Fd3m space group to describe the structure of

the lithiated phase. This space-group takes into account only the average structure. There exists some weak peaks at angles 21.22, 31.70 and $34.08(2\theta)$ which can be approximately indexed as the forbidden reflections (200), (221-300) and (310), respectively; This fact may indicate that some type of order is established giving rise to a superstructure, probably with a weak tetragonal distortion. We have not tried to propose any model because the quality of the data does not permit us to go further. In spite of a poorer R_{wp} index, no pattern region was excluded in the 2θ (14° to 100°) interval.

3. Structural models for $\text{Li}_x\text{Fe}_3\text{O}_4$. Single-phase results

Previously reported data on $\text{Li}_x\text{Fe}_3\text{O}_4$ [13] show that the 16d octahedral subarray of the spinel structure (Fe_3O_4) remains unchanged by lithium incorporation. For x higher than some small critical concentration (x_c), a cooperative displacement of the tetrahedral Fe-ions towards the empty 16c octahedral sites of the spinel Fd3m space-group takes place, leading to a defective rock-salt structure. The Li-ions are inserted in the remaining 16c positions up to $x = 1$. For $2 \geq x > 1$, the Li-ions can occupy the tetrahedral 8a or 48f available sites.

These results have been obtained from a conventional analysis of the X-ray diffraction data together with analysis of the open-circuit voltage measurements. Therefore, it seems worthwhile to reinvestigate the X-ray diffraction data of this compound (not well crystallized), by using the Rietveld method on the basis of the following models:

- (i) $(\text{Li}_{x-1}\text{Fe}_y)_{8a}(\text{LiFe}_{1-y})_{16c}(\text{Fe}_2)_{16d}\text{O}_4$
- (ii) $(\text{Li}_{x-1-y}\text{Fe}_y)_{8a}(\text{Li}_{1+y}\text{Fe}_{1-y})_{16c}(\text{Fe}_2)_{16d}\text{O}_4$
- (iii) $(\text{Li}_{x-1-y})_{8a}(\text{Li}_y)_{48f}(\text{LiFe})_{16c}(\text{Fe}_2)_{16d}\text{O}_4$

In Table I we summarize the calculated values of y , a , u , B_{ov} , R_{wp} , R_E and R_B , in the single-phase refinements for the three models. y gives the cationic distribution, a and u are the lattice and the oxygen parameters respectively. B_{ov} (nm^2) is the overall temperature factor, R_{wp} , R_E , and R_B are the quality-of-fit parameters: R -weighted, R -expected, and R -Bragg. In all cases the value $x = 1.7$ obtained from the chemical analysis, was assumed.

In Fig. 1 we show the fitted X-ray diffraction pattern for Model (i) together with the pattern difference between the observed and calculated data. The inspection of this figure clearly reveals a systematic displacement towards lower angles of the calculated pattern with respect to the experimental one. In addition, the computed intensity of the (220) reflection is lower than the observed one, suggesting that the occupation factor of Fe-ions in the tetrahedral 8a-sites should be higher than the value obtained from the fit, which is constrained by the chemical composition. The fits of Models (ii) and (iii) reveal the same features. In addition, Model (iii) leads to an unacceptable negative occupation factor for lithium in the 48f sites.

On the basis of the R indices it is not possible to discriminate between these different models. Moreover, all these results show that one-phase models do

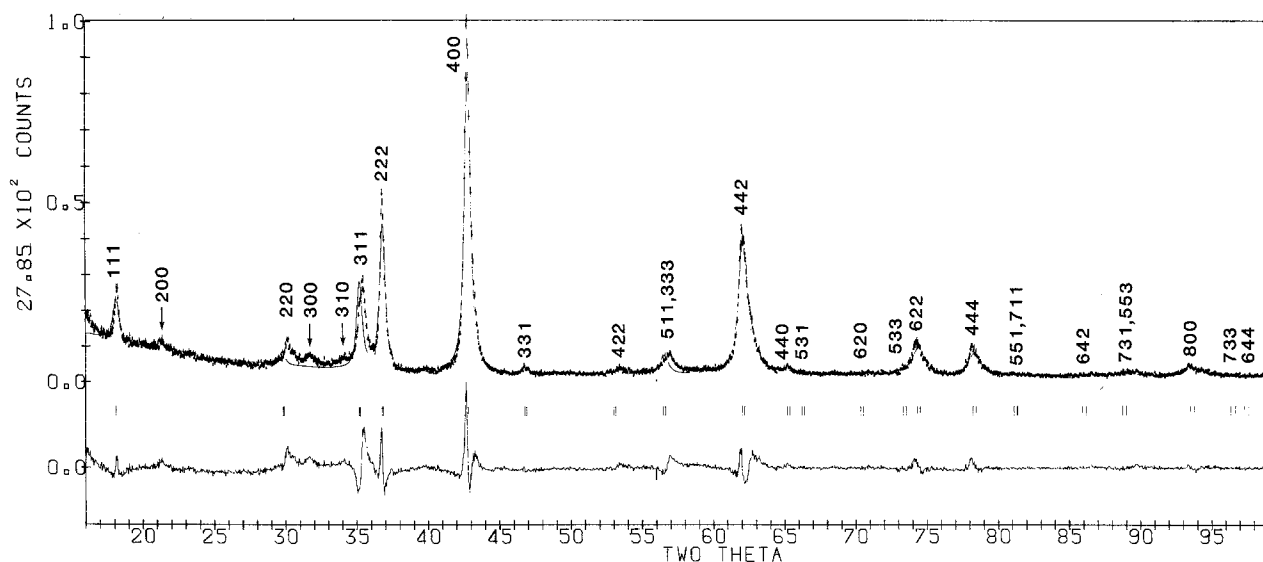


Figure 1 X-ray diffraction pattern of $\text{Li}_x\text{Fe}_3\text{O}_4$, fitted with the single-phase model (i). Arrows indicate forbidden reflections in $\text{Fd}3\text{m}$ space group (see text).

not match the experimental data, and suggest the presence of a secondary phase, probably magnetite.

The Mössbauer spectrum (Fig. 2) of the sample confirms the presence of the secondary phase. The relevant feature of this spectrum is the coexistence of a magnetically ordered phase together with a paramagnetic one. We have calculated from the absorption areas, that the magnetic phase is 16(2)% of the total amount of sample and its Mössbauer parameters (isomer shift, quadrupole splitting and hyperfine magnetic field) are very similar to those found in pure magnetite [14]. A detailed discussion of the Mössbauer results can be found elsewhere [15]. Therefore, we conclude that the sample contains two phases, one very probably being pure magnetite. Consequently, we are forced to refine the diffraction pattern assuming the presence of two phases.

4. Two-phase model

We have started from the assumption that no Fe-ions are present in tetrahedral 8a-sites in the lithiated phase [10] and the octahedral 16c positions are fully occupied. The remaining 0.7 Li being incorporated in 8a sites. For the pure magnetite phase, the lattice parameter ($a = 0.8395 \text{ nm}$) and the oxygen parameter ($u = 0.254$) [16] were used as fixed parameters in the fitting. In the first step we have also assumed that the overall isotropic temperature factor and the half-width parameters are the same for both phases.

When using this model the R_{wp} index dropped to 14.88. The remarkable lower value obtained for R_{wp} confirms the presence of Fe_3O_4 in the sample. The

concentration of magnetite obtained from Equation 3 gives a value of 16.1(5)%. The error of this value was estimated by applying the standard propagation error methods, and perhaps, they give an unrealistic small error. We will discuss this point later. This concentration is in very good agreement with the Mössbauer result. Therefore, it follows that the actual lithium concentration in the lithiated phase must be corrected from the value $x = 1.7$ to $x = 2.0$.

Accordingly, the fitting process has been repeated using $x = 2.0$ and the same constraints in the adjustable set of parameters. As expected, no significant difference in the R_{wp} index has been observed ($R_{\text{wp}} = 14.84$).

In Table II we summarize the obtained results. The symbols (A) to (D) are used to indicate the refinements with the following constraints: (A) $B_1 = B_2$ and $HW_1 = HW_2$, (B) $B_1 \neq B_2$ and $HW_1 = HW_2$, (C) $B_1 = B_2$ and $HW_1 \neq HW_2$, (D) $B_1 \neq B_2$ and $HW_1 \neq HW_2$, where B and HW stand for isotropic temperature factor and half-width parameters of phase i.

In Fig. 3 we show the Rietveld-refined pattern together with the difference pattern between the experimental and the calculated profile using $x = 2.0$ and constraints (A). The improved quality of the fit with respect to the fit obtained with a single-phase model (Fig. 1) can be clearly appreciated.

The inspection of the data in Table II reveals some interesting features that should be emphasized.

1. When any set of constraints is relaxed, a different x_{M} value is obtained. These x_{M} values do not overlap

TABLE I Parameters obtained from the fit of the profile of the XRD pattern

Model	a (nm)	u	y	B_{ov} (nm^2)	R_{wp}	R_{E}	R_{B}
(i)	0.8461(1)	0.2510(7)	0.175(6)	0.007(1)	18.28	7.73	4.83
(ii)	0.8461(1)	0.2510(7)	0.192(6)	0.007(1)	18.28	7.73	4.82
(iii)	0.8460(1)	0.254(1)	-2.577(1)	0.009(2)	18.75	7.73	5.01

The symbols (i), (ii), (iii) refer to the different structural models discussed in the text.

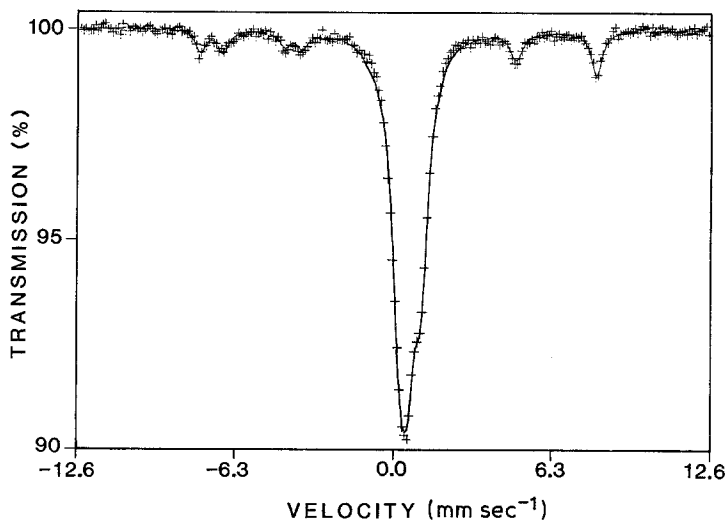


Figure 2 Room temperature Mössbauer spectrum of $\text{Li}_x\text{Fe}_3\text{O}_4$.

within their standard deviation. However, the standard deviation of the Mössbauer result includes all the different x_M values obtained by XRD.

2. When the constraint $B_1 = B_2$ is relaxed, a negative B_{ov} is obtained for the magnetite phase. However, temperature factors are generally rather unreliable in the X-ray Rietveld refinements, and even more in the present situation of a strong peak overlapping.

3. When the constraint $H_1 = H_2$ is relaxed, magnetite peaks appear to be larger than those corresponding to the lithiated phase. Despite the difficulty of interpretation, this fact seems reasonable when account is taken of the delithiation process, which takes place at the surface of the grains and leads to very small Fe_3O_4 crystallites.

4. The introduction of the $B_1 = B_2$ and $H_1 = H_2$ constraints, despite their lack of physical significance, leads to a Fe_3O_4 concentration very close to the value obtained from Mössbauer spectroscopy [15].

Despite the low scattering factor of lithium, it may be argued that the fit for $x = 1.7$ can be dependent on the assumption that the 16c positions are fully Li-occupied and therefore that the concentration of about 16% of magnetite may no longer be valid. In order to investigate this effect we have refined the data

with the two-phase model, but using a different lithium concentration (0.6), and allowing for a free Li-distribution over the available 8a and 16c sites. This particular concentration is suggested by the isomer shifts of the low-velocity lines in the Mössbauer spectrum and the deduced $\text{Fe}^{2+}/\text{Fe}^{3+}$ ratio [15]. Our results show that R_{wp} does not vary appreciably with the lithium distribution, as expected: $R_{wp}[(\text{Li}_{0.6})_{8a}] = 15.23$, $x_M = 15.3(5)$, and $R_{wp}[(\text{Li}_{0.6})_{16c}] = 15.31$, $x_M = 17.1(5)$.

Therefore, we can conclude that the concentration of magnetite (16%) deduced from the $x = 1.7$ case is practically independent of the lithium concentration and distribution.

5. Conclusions

The results obtained in this study show that it is not possible to discriminate between different models of lithium distribution, due to its low scattering factor with respect to those of the iron and oxygen ions. Moreover, the true lithium concentration of the lithiated phase remains unknown. These facts breakdown the possibility of solving the structure of $\text{Li}_x\text{Fe}_3\text{O}_4$ from the X-ray powder diffraction data.

However, from these data two important conclusions

TABLE II Parameters obtained from the fit of the profile of the X-ray pattern, with a two-phases model

	(A)	(B)	(C)	(D)
P	17	18	20	21
R_{wp}	14.84	14.82	14.52	14.50
R_E	7.73	7.72	7.72	7.72
R_B	4.90, 4.54	4.57, 4.39	5.26, 4.65	5.13, 4.59
B (nm)	0.004(1)	0.005(1), -0.001(3)	0.0035(8)	0.004(1), -0.001(3)
U	1.8(2)	1.7(2)	1.5(2), 5(2)	1.4(2), 6(2)
V	-0.9(2)	-0.9(2)	-0.6(2), -4(1)	-0.6(2), -5(2)
W	0.24(4)	0.23(4)	0.15(3), 1.0(2)	0.15(3), 1.2(3)
a (nm)	0.84636(8)	0.84640(9)	0.8464(1)	0.8465(1)
u	0.2512(8)	0.2511(8)	0.2510(7)	0.2509(7)
K_1 (10^6)	48.2(8)	48.9(8)	46.7(7)	47.2(9)
K_2 (10^6)	9.2(2)	8.6(3)	10.8(3)	10.3(5)
x_M (%)	15.6(5)	14.6(6)	18.3(6)	17.5(1.0)

U , V , and W are the coefficients of the line-width function. P is the number of fit parameters, K_1 and K_2 stand for the scale factor of $\text{Li}_{2.0}\text{Fe}_3\text{O}_4$ and Fe_3O_4 , respectively. x_M (%) is the weight fraction of magnetite. The second number in a given row and array is the corresponding parameter of magnetite. The remaining symbols have the same meaning as those in Table I. (A), (B), (C) and (D) refer to different sets of constraints in the fitting procedure.

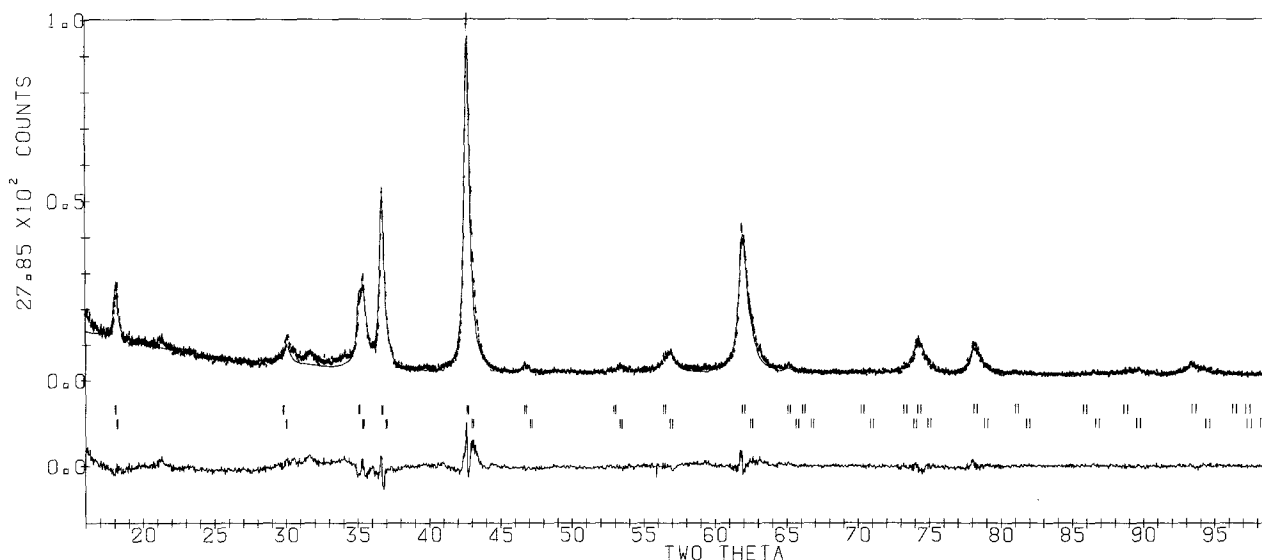


Figure 3 X-ray diffraction pattern of $\text{Li}_x\text{Fe}_3\text{O}_4$, fitted with the two phase model (A).

can be extracted. The first is that if the classical quantitative analysis methods cannot be used (very strong overlapping, standards cannot be prepared, . . .) the Rietveld method can be successfully used, even if the structures are only partially known.

In addition, it should be noticed that the x_M values obtained from any refinement run (different structural models and different constraint sets) are in agreement (within the standard deviation) with the value deduced from Mössbauer spectroscopy.

The second conclusion refers to the evaluation of the estimated error of the magnetite concentration x_M from XRD. Due to the strong correlation between fitting parameters, the errors evaluated by the standard propagation formula are unrealistic, and in order to include the experimental concentration (from the Mössbauer results), the XRD standard deviation of x_M should be multiplied by a factor of 3.

References

1. H. M. RIETVELD, *J. Appl. Cryst.* **2** (1969) 65.
2. A. ALBANATI and B. T. M. WILLIS, *ibid.* **15** (1982) 361.
3. R. A. YOUNG and D. B. WILES, *ibid.* **15** (1982) 470.
4. C. J. HOWARD, *ibid.* **15** (1982) 615.
5. A. IMMIRZI, *Acta Cryst.* **B36** (1980) 2378.
6. G. A. MACKENZIE, R. W. BERG and G. S. PAWLEY, *ibid.* **B36** (1980) 1001.
7. D. B. WILES and R. A. YOUNG, *J. Appl. Cryst.* **14** (1981) 149.
8. P. J. BENDALL and M. W. THOMAS, AERE Harwell MPD. Internal Report HL81/101 (1981).
9. P. E. WERNER, S. SALOMÉ, G. MALMROS and J. Q. THOMAS, *J. Appl. Cryst.* **12** (1979) 107.
10. M. M. THACKERAY, W. I. F. DAVID and J. B. GOODENOUGH, *Mat. Res. Bull.* **17** (1982) 785.
11. R. J. HILL and C. J. HOWARD, *J. Appl. Cryst.* **18** (1985) 173.
12. A. GUINIER, "Theorie et Technique de la Radio-cristallographie" (Dunod, Paris, 1964).
13. M. M. THACKERAY, W. I. F. DAVID and J. B. GOODENOUGH, *J. Solid State Chem.* **55** (1984) 280.
14. B. J. EVANS and S. HAFNER, *J. Appl. Phys.* **40** (1969) 1412.
15. J. FONTCUBERTA, J. RODRIGUEZ, M. PERNET, G. LONGWORTH and J. B. GOODENOUGH, *J. Appl. Phys.* **59** (1986) 1918.
16. N. N. GREENWOOD, "Cristales iónicos, defectos reticulares y estructura" (Alhambra, Madrid, 1970).

Received 25 March
and accepted 21 July 1986